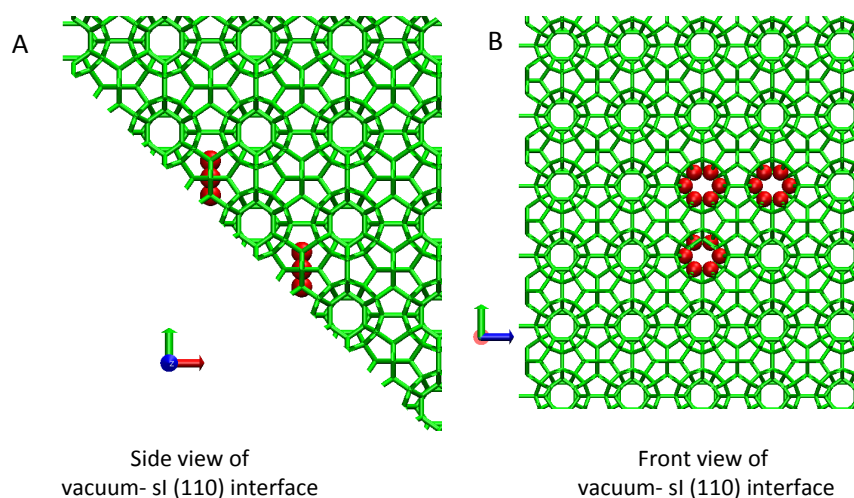


## Structure of the Ice-Clathrate Interface

Andrew H. Nguyen,<sup>1</sup> Matthew A. Koc,<sup>1,2</sup> Tricia D. Shepherd,<sup>2</sup> Valeria Molinero<sup>1</sup>

<sup>1</sup>*Department of Chemistry, The University of Utah, 315 South 1400 East, Salt Lake City, UT 84112-0850,* <sup>2</sup>*Westminster College, 1840 South 1300 East, Salt Lake City, UT 84105*



**Figure S1. Orientation of the six-member water rings with respect to the (110) plane of sI clathrate.** Three neighboring six member water rings are highlighted with red balls. Panel S2A shows the side view of the (110) plane exposed to vacuum, while panel S2B display the top view of the same plane. The (110) plane of sI contains a higher density of hexagonal rings than the (100) plane; however, the hexagonal rings are oriented at 45° to the (110) plane.

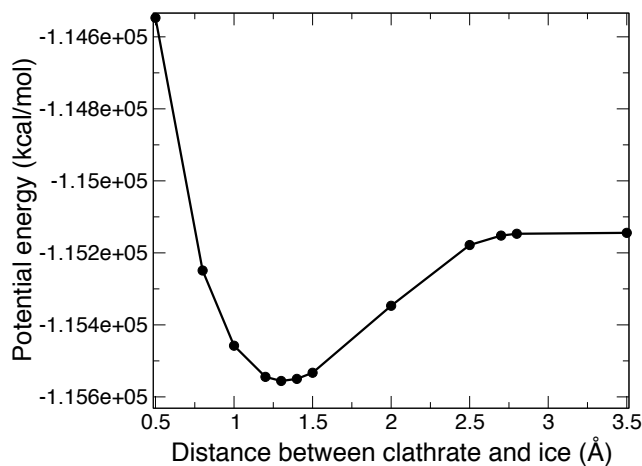


**Figure S2. Potential energy as a function of the distance between the outermost water layer in rigid ice and clathrate crystals.** The ice-clathrate system consists of 10151 mW water molecules. We align the basal plane of hexagonal ice with the (100) plane of sI clathrate as indicated in Section 2B “Systems” and vary the distance. Single point calculations of the potential energy of the ice clathrate system were performed, without any minimization, at each distance. The minimum in potential energy occurs at 1.3 Å.

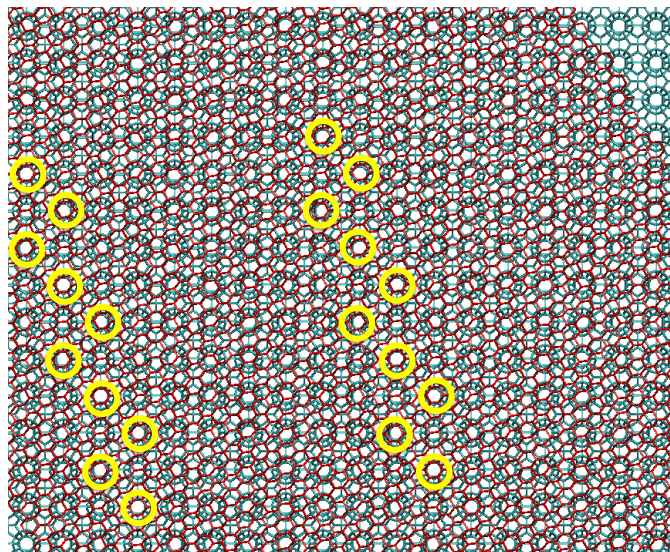


**Figure S3. Overlay of the prismatic plane of hexagonal ice and the (100) plane of sI clathrate.** Ice shown with red sticks and clathrate with cyan sticks. The yellow circles mark the aligned hexagonal water rings between ice and clathrate. The closest distance between nearest hexagons is 15 Å, the long distance between hexagons across the x axis is 72.1 Å.

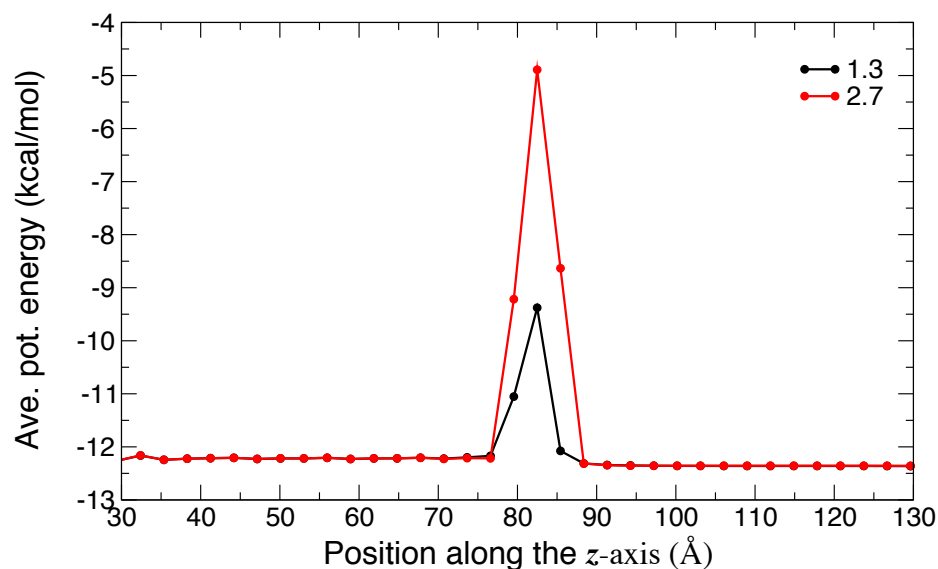


**Figure S4. Average potential energy of the minimized ice-clathrate interface.** The black curve represents the potential energy as a function of distance when positioning the ice and the empty clathrate at 1.3 Å (the minimum of the non-minimized potential energy distance), while the red curve represent the minimized potential energy at 2.7 Å (close to the distance of O-O bond in water crystals). The differences in potential energy of the center of the interfacial water with respect to ice are 2.83 kcal/mol and 7.53 kcal/mol for 1.3 Å and 2.7 Å, respectively, higher than the difference between ice and equilibrated liquid water at the melting point.

**Table S1. Density of direct contacts of the aligned ice-clathrate interface after minimization of the potential energy.** The density of *direct contacts* for the minimized system was measured as a water molecule classified as clathrate within 3.5 Å of a water molecule classified as ice, or vice versa. Percentages of surface clathrate or ice molecules in direct contact with molecules of the other crystal are listed in parentheses. The surface density of water molecules at the (100) plane of sI clathrate hydrate is 7.2 nm<sup>-2</sup>.

Ice plane in contact with (100) plane of sI clathrate.	Surface density of molecules in the ice plane (nm <sup>-2</sup> )	Density of direct contacts of ice molecules (nm <sup>-2</sup> )	Density direct contacts of clathrate molecules (nm <sup>-2</sup> )
Basal plane of ice	7.6	2.6 (29%)	3.3 (40 %)
Prismatic plane of ice	6.7	2.5 (28 %)	3.3 (44%)
Secondary prismatic plane of ice	6.0	2.4 (19 %)	1.9 (35 %)

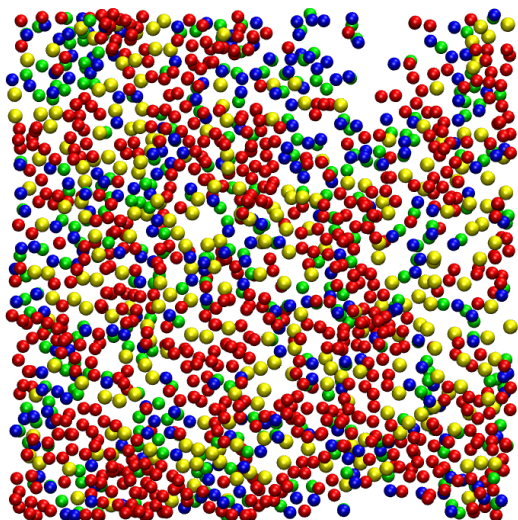


**Figure S5: Direct and mediated contacts at the I3 interfacial transition layer.** The blue beads represent ice molecules in direct contact with clathrate, green beads represent clathrate molecules in direct contact with ice. Red and yellow beads represent liquid-like water in the disordered layer: the yellow beads mediate liquid-like water molecules with both ice and clathrate molecules within 3.5 Å (these are called mediated contacts).

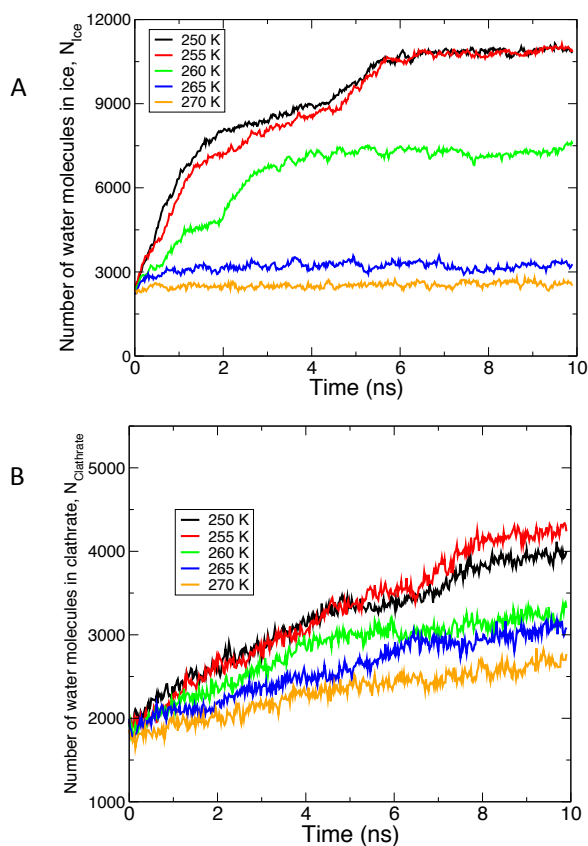


**Figure S6. Competing growth of clathrate hydrates and ice from a common solution at temperatures ranging from 250 to 270 K.** The top panel shows the number of water molecules in the ice phase as a function of time. The bottom panel shows the number of water molecules in the clathrate phase as a function of temperature. Growth of the clathrate is limited by diffusion of guest molecules to the growing surface.



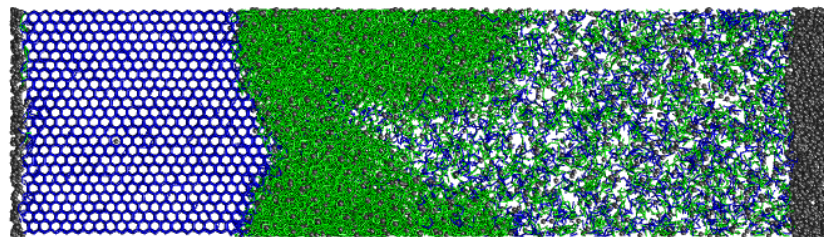


**Figure S7: Growth of the nucleated clathrate in the presence of secondary-prismatic plane of hexagonal ice at 100 atm and 260 K.** Additional 50 ns simulation was performed from the final configuration shown in figure 10B of section 3D, resulting in less rugged ice-clathrate interface. The blue lines represents molecules classified as ice, green as clathrate and gray beads show the guest molecules. Liquid water is not shown here. The interface becomes flatter after long simulation time. The interface exposed to the clathrate phase in this figure is the secondary-prismatic plane of hexagonal ice.

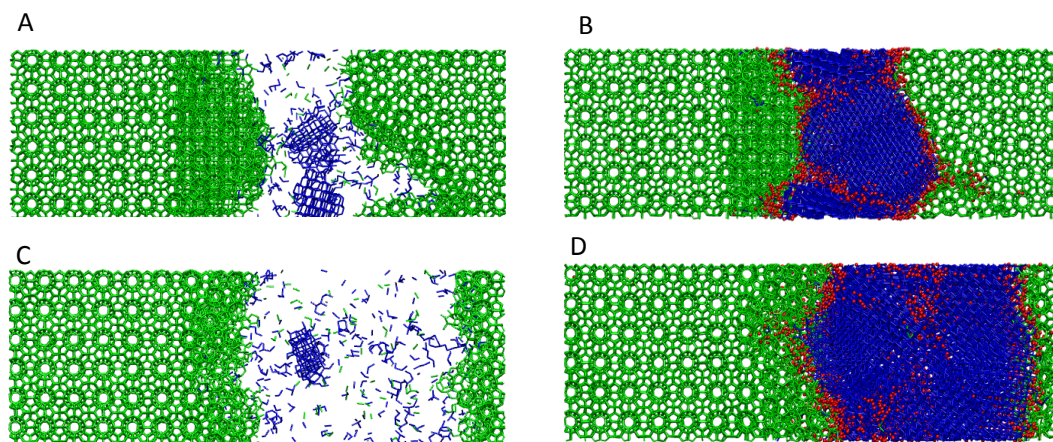


**Figure S8: Ice-clathrate interface formed by nucleation of ice in the presence of the empty clathrate.** Initially, the exposed plane is the (100) face of empty sI clathrate. The (100) plane of empty sI clathrate undergoes cross nucleates to sII clathrate before ice nucleates in the simulations at 205 and 208 K. The water molecules identified as clathrate are shown in green, and those in ice are shown in blue. Liquid water molecules are shown only in the final configurations (B and D), with red balls. The emerging ice nuclei are within the liquid phase. The upper panels show snapshots of the simulation at 205 K and 1 atm: the emerging ice nucleus in solution (A) and the ice-clathrate interface formed after 10 ns simulation (B). The lower panels show snapshots of the ice nucleation at 208 K and 1 atm: the budding ice nucleus in solution (C), and the ice-clathrate interface after 10 ns (D).